Supplementary Information/Appendix

"Circularly Polarized Fabry-Perot Cavity Sensing Antenna Design using Generative Model"

K. Yasmeen, K. V. Mishra, A. Subramanyam, and S. S. Ram

In this document, we discuss the experiments that were performed to determine the design parameters of the proposed algorithms and GAN network hyper-parameters. In section I, we describe the network architecture. In section II, we explain the design parameters of the proposed antenna design, and in section III, we present the additional measurement experiments.

I. Network Architecture

We consider the GAN network hyper-parameters, such as the number of layers, the number of nodes, batch size, and the learning rate. For the quantitative comparison, the normalized mean square error (NMSE) is computed between the ground truth (y) and estimated antenna characteristics ($\hat{y}$) using

$$NMSE = \frac{\|y - \hat{y}\|_2^2}{\|y\|_2^2}. \tag{1}$$

The NMSE is computed across test samples of gain, axial ratio, and return loss respectively. The quantitative comparison of the techniques for all the test cases is summarized below.

We experimented with different numbers of layers and nodes in the generator and critic networks. Table I summarizes the average NMSE for various network structures for 270 training samples and 30 test samples. Here, for the generator, we have performed the experiments for 2 and 3 hidden layers with different combinations of nodes such as 128-256, 128-256-512, provided in Table I. Similarly, we have considered a critic with two hidden layers with different numbers of nodes. Here, we have considered a learning rate of 0.0005 and a batch size of 16.

Table I: Average NMSE for different network structures

Generator	Critic	Gain	Axial Ratio	Return Loss
128-256	512-256	0.23	0.1	0.2
128-128	512-256	0.24	0.1	0.24
128-256-512	512-256	0.23	0.05	0.2
128-256-512	256-128	0.24	0.05	0.23
128-256-512	128-64	0.21	0.08	0.25

We note that the generator 128-256-512 and the critic 512-256 yield lower average NMSE for gain, axial ratio, and return loss. We also tried different learning rates and batch sizes; see Table II. We have fixed the batch size to 16 for analyzing the performance of the model with the variation of the learning rate. Similarly, we fixed the learning rate to 0.0005 and varied the batch size as shown in Table II. The parameters were heuristically selected, and the total number of iterations was set to 10000.

Table II: Average NMSE for various hyper-parameter values

Hyper Parameter	Value	Gain	Axial Ratio	Return Loss
Learning rate	0.0005	0.23	0.05	0.2
Learning rate	0.0002	0.2	0.08	0.24
Learning rate	0.01	0.4	0.3	0.43
Batch size	32	0.21	0.08	0.25
Batch size	16	0.23	0.05	0.2

We show the change in the generator and critic loss functions with training iterations in Fig.1. We observe that generator loss converges after 4000 epochs. The critic losses converge around 0.5, indicating that training convergence has been achieved [1], [2].

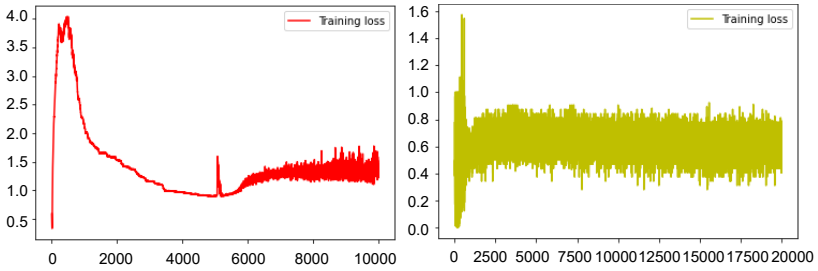

Fig. 1. Variation of (a) generator and (b) critic loss during training.

We have compared our optimized GAN with the best MLP and CNN architectures. The best MLP architecture that we could find consists of two layers with 256-512 nodes with 32 batch sizes and a 0.0002 learning rate. The best CNN architecture that we found consists of 2 layers with 64 filters in each layer with kernel size, 3 batch size 32, and 0.0002 learning rate.

Table III: NMSE of antenna characteristics

Networks	Gain	Axial Ratio	Return Loss
MLP	0.3	0.09	0.27
CNN	0.28	0.08	0.26
GAN	0.23	0.05	0.2

We observe that the GAN is still able to perform better in comparison to MLP and CNN architecture.

II. Fabry Perot Cavity (FPC) System Model

FPC antennas are high-gain single-feed antennas with a dielectric cavity enclosed by a metal ground plane on one side and a PRS on the other. A primary source of excitation is introduced within the cavity that gives rise to EM waves. The height of the cavity is carefully chosen such that the multiple reflections within the cavity are in phase with each other when they emanate from the antenna, thereby enhancing the gain of the primary radiator. The polarization of the resulting radiation is determined by either the polarization of the primary radiating source or the unit cell in the PRS.

In this work, we consider a basic FPC structure (Fig.2a), whose primary radiator is a patch antenna with a single-feed mounted on a substrate layer of Rogers 4350B material of thickness $sbth$. The patch is designed to resonate at 2.4 GHz and is impedance matched to 50 Ω through a multi-stage quarter-wave transformer (Fig.2b(i)). The other side of the substrate is a partial ground metal plane of copper (Fig.2b(ii)). The patch radiates into a polystyrene-based dielectric cavity of h thickness and dielectric constant of 1.05. The other end of the cavity is enclosed by a superstrate layer also of Rogers 4350B material of thickness $spth$. The inner side of the superstrate is printed with a periodic array of 4×4 unit cells in copper to form a PRS (Fig.2b(iii)). Each unit cell of the PRS is a rectangular loop with a diagonal.

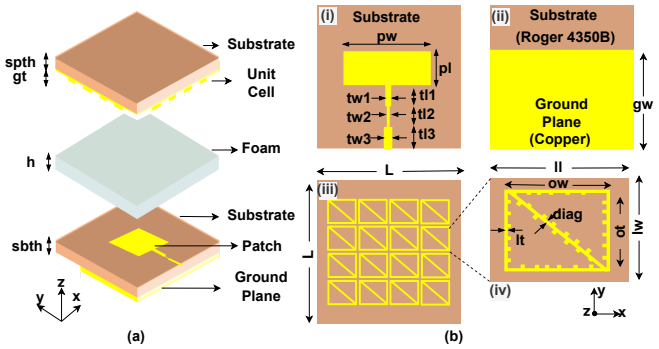

Fig. 2. (a) Three-dimensional view of the circularly polarized FPC antenna. (b) Top-view of (i) patch with a three-stage quarter-wave transformer, (ii) partial reflecting ground plane, (iii) partially reflecting superstrate containing 4×4 array of uniform unit cells with the diagonal, (iv) and unit cell with peripheral roughness.

Table IV lists the dimensions for this basic antenna structure; these values remain fixed across all candidate designs. Then, peripheral roughness is introduced to the metallic edges along each dimension of the unit cell through 36 square metal bricks of 0.5 mm $\times$ 0.5 mm dimensions (Fig.2b(iv)).

Table IV: Dimensions of Basic FPC Structure

Dimensions	Values (mm)	Dimensions	Values (mm)
L	120	tl1	17
gt	0.035	tl2	17
sbth	0.76	tl3	9.5
tw1	2.89	pl	33
tw2	1.63	pw	63
tw3	4.65	gw	87
ow	23.1	ll	26.25
ot	19.9	lw	22
spth	1.524	diag	1.26
h	6.05	lt	1.05

The positions of the metal bricks along the peripheries of the rectangular loop become the degrees of freedom for further reducing the axial ratio while enhancing the gain and bandwidth of the antenna structure. The position of each brick is indicated in two-dimensional Cartesian coordinates, with the origin assumed to be at the left lower corner of the unit cell. The antenna system with each unique unit cell design is then simulated in CST Microwave Studio. Since this is a three-dimensional antenna structure, there are approximately 6.4 million mesh cells for each design. The resulting full-wave EM analysis of the antenna structure is carried out to obtain the gain, return loss, and axial ratio of the structure as a function of frequency from 2 to 3 GHz. The duration of each simulation is approximately 75 minutes. Due to the time-consuming nature of the EM simulations, we explore the use of GAN to train a neural network to serve as a surrogate model. We consider 300 unit cell designs consisting of unique distributions of the metallic bricks and their corresponding antenna characteristics (obtained from CST Microwave Studio) to form the training and validation input-output pairs of the GAN architecture.

III. Additional Measurements

The measurements of gain, return loss, and axial ratio are carried out with a vector network analyzer N9926A and a linearly polarized reference horn antenna (HF907) with known gain characteristics. Quantitative comparisons (Table.V) with FPC and the simple patch further demonstrate the performance enhancements with a GAN-aided design. We consider four antenna characteristics - the gain at the resonant frequency at the antenna boresight, the return loss bandwidth (ZBW), the 5dB AR bandwidth, and the corresponding optimum AR. We observe that the proposed antenna has a wider bandwidth, lower AR, and higher gain than the simple patch.

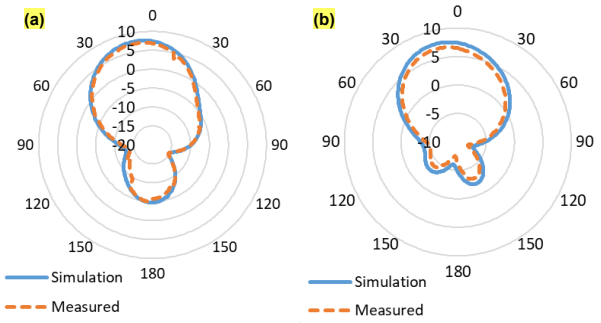

Fig. 3. Variation of (a) H plane and (b) E plane radiation pattern for proposed antenna design at 2.4 GHz

Table V: Comparison with competing antenna structures of antenna characteristics

Antenna	ZBW(MHz)	3dB BW(MHz)	Axial Ratio (dB)	Gain (dBi)
Simple patch	20	-	40	3.4
FPC with PRS	88.5	-	7.6	9.4
GAN-based FPC, rough PRS	269	100	0.4	7.5

In Fig.3, we present the simulated and measured radiation patterns of the proposed antenna structure along the E plane and H plane at the resonant frequency of 2.4 GHz. The proposed antenna also has a wider bandwidth and lower AR with respect to the FPC with smooth PRS, though the gain is slightly lower.

REFERENCES

[1] A. Radford, L. Metz, and S. Chintala, "Unsupervised representation learning with deep convolutional generative adversarial networks," *arXiv preprint arXiv:1511.06434*, 2015.

[2] I. Goodfellow, J. Pouget-Abadie, M. Mirza, B. Xu, D. Warde-Farley, S. Ozair, A. Courville, and Y. Bengio, "Generative adversarial nets," in *Advances in Neural Information Processing Systems*, 2014, pp. 2672–2680.